Chemistry–A European Journal
Research Article
doi.org/10.1002/chem.202302112
Chemistry Europe
European Chemical Societies Publishing
www.chemeurj.org

Hot Paper

Encapsulation in Charged Droplets Generates Distorted Host-Guest Complexes**

Daniel L. Stares,[a] Agnieszka Szumna,*[b] and Christoph A. Schalley*[a]

Dedicated to Wei Jiang. May he rest in peace.

The ability of various hydrogen-bonded resorcinarene-based capsules to bind α,ω-alkylbisDABCOnium (**DnD**) guests of different lengths was investigated in solution and in the gas-phase. While no host-guest interactions were detected in solution, encapsulation could be achieved in the charged droplets formed during electrospray ionisation (ESI). This included guests, which are far too long in their most stable conformation to fit inside the cavity of the capsules. A combination of three mass spectrometric techniques, namely, collision-induced dissociation, hydrogen/deuterium exchange, and ion-mobility mass spectrometry, together with computational modelling allow us to determine the binding mode of the **DnD** guests inside the cavity of the capsules. Significant distortions of the guest into horseshoe-like arrangements are required to optimise cation-π interactions with the host, which also adopt distorted geometries with partially open hydrogen-bonding seams when binding longer guests. Such quasi "spring-loaded" capsules can form in the charged droplets during the ESI process as there is no competition between guest encapsulation and ion pair formation with the counterions that preclude encapsulation in solution. The encapsulation complexes are sufficiently stable in the gas-phase – even when strained – because non-covalent interactions significantly strengthen in the absence of solvent.

Introduction

Electrospray ionisation (ESI) is the most common method of generating gaseous ions as it is soft and proceeds directly from solution.[1] ESI is also capable of accelerating reaction rates,[2] facilitating the self-assembly of supramolecular systems[3] and is even able to form complexes which cannot be observed in solution;[4] a prominent example of this being the serine octamer clusters.[5] An interesting aspect of ESI is that the charged droplets which form offer an environment where charge neutrality is violated enabling novel chemistry to occur. This can potentially be useful for hosts binding charged guests as the counterion(s) will be stripped away obviating any ion pairing issues that may be present in solution, enhancing binding by enabling direct interaction of the naked ion with the host. In addition, as the droplets undergo desolvation, there is a concentration increase which further facilitates binding.[6] Because of these factors, it is possible to generate unusual host-guest complexes and binding modes not observed in solution. These complexes then survive transfer into the gas-phase due to the strengthening of most non-covalent interactions in the absence of solvent.[7]

To study the unique complexes which form in charged droplets, it is necessary to utilise mass spectrometry (MS). As mass-to-charge ratio (*m/z*) alone does not provide details on an ion's structure, the investigation requires more advanced MS techniques such as collision-induced dissociation (CID), gas-phase hydrogen deuterium exchange (HDX), and ion-mobility mass spectrometry (IMS). With these techniques, it is possible to elucidate structural and energetic information of an ion and thus gain insight into the chemistry occurring in the charged droplets.

Resorcinarenes are widely used hosts which can bind cations thanks to an electron-rich bowl-shaped cavity.[8] Resorcinarenes can self-assemble into dimeric[9] and hexameric capsules[10] and offer great versatility owing to potential modifications of both their upper and lower rims, forming diverse hydrogen-bonded,[11] metallo-supramolecular,[12] anion-based,[13] and halogen-bonded capsules.[14] Such modular design allows for the modification of cavity size and function potentially encapsulating a range of guests both in terms of size[15] and class of guest, with anion binding even possible with the appropriate modifications.[16]

Herein, we report the encapsulation of different length dicationic α,ω-alkylbisDABCOnium (**DnD**) guests into hydrogen-

[a] D. L. Stares, Prof. Dr. C. A. Schalley
Institut für Chemie und Biochemie
Freie Universität Berlin
Arnimallee 20, 14195 Berlin (Germany)
E-mail: c.schalley@fu-berlin.de

[b] Prof. A. Szumna
Institute of Organic Chemistry
Polish Academy of Sciences
Kasprzaka 44/52, Warsaw (Poland)
E-mail: agnieszka.szumna@icho.edu.pl

[**] A previous version of this manuscript has been deposited on a preprint server (https://chemrxiv.org/engage/chemrxiv/article-details/648c70714f8b1884b7638f6f).

Supporting information for this article is available on the WWW under https://doi.org/10.1002/chem.202302112

bonded resorcinarene-based capsules. No interaction was seen in solution by nuclear magnetic resonance (NMR), but encapsulation could be promoted via ESI, including guests which should be too long to fit inside the cavity. In these cases, encapsulation requires large distortions of the host-guest complexes which could be uncovered by a combination of MS and computational modelling. The encapsulation of these guests is a prototypical example of chemistry occurring under conditions violating electroneutrality, forming complexes not observed in solution. This offers qualitative insight into the enhanced non-covalent interactions in the absence of solvent and highlights the three very different environments the complexes encounter: solution, charged droplets and the gas-phase.

Results and Discussion

The cavitands are synthesised by acylhydrazone formation betweena hydrazide containing strand to a tetraformylated resorcinarene precursor (Scheme 1) (full synthetic details and characterisation can be found in the Supporting Information). Previously, cavitands capable of dimerising via N–H···O hydrogen bonds were prepared by attaching mono-, di-, tri- and tetrapeptide strands to the upper rim of resorcinarenes.[17] It was expected that the longer strands would result in larger cavities when dimerising. However, cavity size did not change as the capsules were only engaging the first amino acid for intermolecular hydrogen bonding leaving the terminal ends of the strands unbound.

In the current study, the strand was shortened to an acetyl moiety which resulted in the formation of a new hydrogen-bonded dimer of this type (**1**) (Figure 1a). Dimer formation of **1** was supported by both Diffusion-Ordered Spectroscopy (DOSY) and Rotating Frame Overhauser Enhancement Spectroscopy (ROESY) (Figures S3 & S4) and suggests a binding motif involving a continuous seam of eight hydrogen bonds propagating around the capsule (Figure 1a). Comparing HF-3c optimised models of $\mathbf{1}_2$ (Figure 1a) and the previously reported phenylalanine peptide capsule $\mathbf{2}_2$ (Figure 1b)[17a] shows that shortening the chain to an acetyl moiety reduces the dimensions of the capsule and thus $\mathbf{1}_2$ and $\mathbf{2}_2$ can be used to monitor the effect of cavity size on guest binding.[18] DABCO heads connected by alkyl chains of different lengths (**DnD**, n = 2–12, Figure 1c) were used as guests which should bind with the electron-rich resorcinarene cores via cation-π interactions.[19] The guest's double charge allows interaction with both hemispheres of $\mathbf{1}_2$ and $\mathbf{2}_2$ whilst Coulomb repulsion between the two charges should favour full extension of the **DnD** enabling an assessment of guest size on binding.

Because of the ring current within the four aromatic rings of the resorcinarene core, encapsulation of the guest into the capsule's cavity would produce clear upfield shifts of the guest's ^{1}H NMR signals. NMR measurements for these compounds were hampered by solubility issues as $\mathbf{1}_2$ and the **DnD**·$(PF_6)_2$ salts were not soluble in the same solvent at the concentrations required for NMR. Solvent mixtures can be used, but this was complicated by the competitive nature of most polar solvents for hydrogen bonding meaning they can only be used in small amounts.[17] A 4:1 chloroform:acetonitrile mixture dissolved $\mathbf{1}_2$ and **D5D**·$(PF_6)_2$ however, no shifts that indicate encapsulation were observed (Figure S11).[20] The same result was obtained when guest salts with tetrakis[3,5-bis(trifluoromethyl)phenyl]borate (**BArF**) counterions were used.[21] **BArF** is less coordinating than PF_6^- and increases solubility in non-polar solvents such that **D9D**·$(\mathbf{BArF})_2$ and $\mathbf{1}_2$ were both soluble in pure dichloromethane (DCM). Still, no interaction between host and guest was observed (Figure S12). No changes were seen when samples were re-measured after several days (Figure S13), nor was interaction seen when measuring with different **DnD**

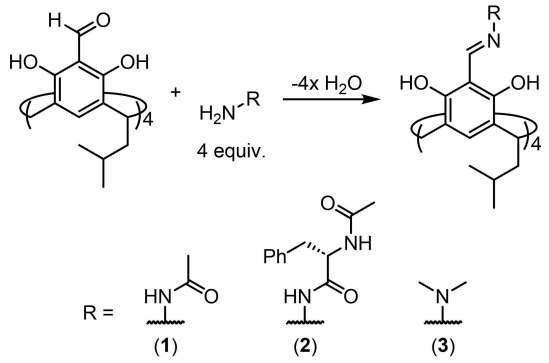

Scheme 1. Formation of the cavitands via acylhydrazone chemistry.[17]

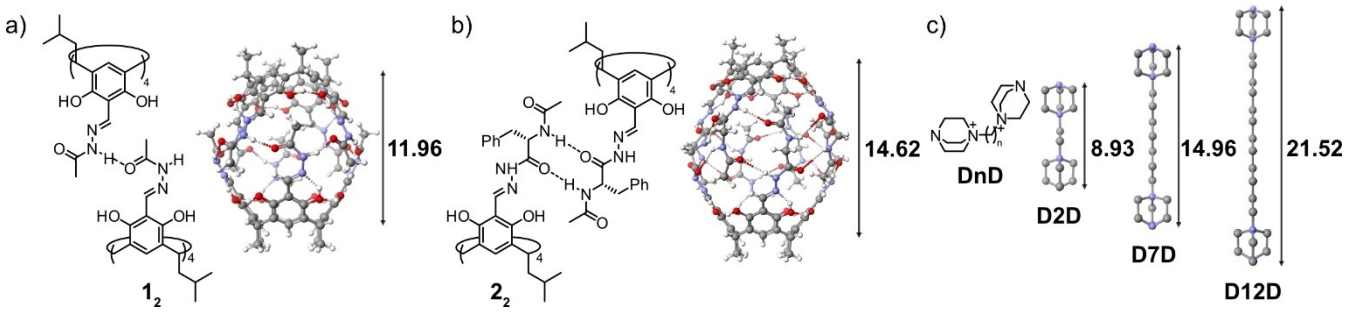

Figure 1. a) Acetylhydrazoneresorcinarene capsule ($\mathbf{1}_2$). b) Phenylalanineresorcinarene capsule ($\mathbf{2}_2$). The distances from lower rim to lower rim are marked in Å. c) $\mathbf{DnD}^{2+}$ guests which should be fully extended due to charge repulsion. The $(CH_2)_3N$–$N(CH_2)_3$ distance is marked in Å. All models were optimised at the HF-3c level of theory.

guests (Figure S14). Thus, from the NMR analysis, it is clear that guest encapsulation does not occur in solution, even in non-competitive solvents such as DCM.

In marked contrast, strong signals for ions corresponding to the dimer/guest complex ($[M_2+\mathbf{DnD}]^{2+}$) were observed via ESI-MS for all guests with both $\mathbf{1_2}$ and $\mathbf{2_2}$ (Figures S16–21), even when measuring samples in competitive solvents such as acetonitrile (Figure S22–24). As the complexes do not exist in solution before ionisation and we can safely rule out their formation in the gas-phase after the ESI process, the only conclusion is that the encapsulation has occurred in the positively charged droplets *during* ESI. In ESI, ions are formed via the desolvation of analyte ions in charged droplets (Figure S15).[22] These droplets contain an excess of positive charges from guests without counterions and thus, the effect of ion pair formation is waived. This allows interactions between the naked cation and the capsule and when coupled with the concurrent increase in concentration during desolvation, enables encapsulation that cannot be seen by NMR. Consequently, such encapsulation represents supramolecular chemistry occurring under conditions violating electroneutrality.

Although this clear-cut difference between NMR and MS results can be understood, some **DnD** should be too long to bind so it is still surprising to see interactions between $\mathbf{1_2}$ or $\mathbf{2_2}$ and *all* guests. A straightforward explanation would be that this is due to a non-specific interaction between host and guest occurring during ESI, i.e., the **DnD** guests are binding externally rather than truly being encapsulated. To investigate this, the disassembly of the ions was studied via collision-induced dissociation (CID) where ions are accelerated by an electric field and collided with a neutral buffer gas. This converts some of the ions' kinetic energy into internal energy eventually leading to fragmentation, if this energy is sufficiently high (Figure 2a).[23] CID of the mass-selected $[M_2+\mathbf{DnD}]^{2+}$ ions resulted in loss of one cavitand unit to the $[M+\mathbf{DnD}]^{2+}$ ion before further dissociation of the guest (Figures 2b and c). The intact free guest was not observed for the shorter chain length guests ($n \leq 3$) due to the strong repulsion of the two charges in the gas-phase over such a short range (Figure S26),[24] but the initial cavitand loss was seen for all guests and hosts. This dissociation pathway already supports the hypothesis of guest encapsulation over non-specific binding as guest loss would certainly dominate, if the guest was non-specifically bound to the outer surface of the capsule. The relatively high collision voltage required to induce dissociation also speaks against non-specific binding as such an interaction would only be weak and the non-specific complexes would thus dissociate at much lower collision voltages.[25] A relative ranking of gas-phase stabilities can be determined by survival yield (SY) plots which can be constructed by calculating parent ion relative intensity at increasing collision voltages and plotting the two against each other.[26] This produces a sigmoidal curve where the inflection point represents the voltage at which the parent ion intensity is half of the total intensity ($SY_{50\%}$), with higher $SY_{50\%}$ values indicating greater stability (Figure S27). For $[\mathbf{1_2}\subset\mathbf{DnD}]^{2+}$, a similar stability is observed for $n=2$–5 followed by a gradual and consistent decrease in $SY_{50\%}$ values at longer chain lengths

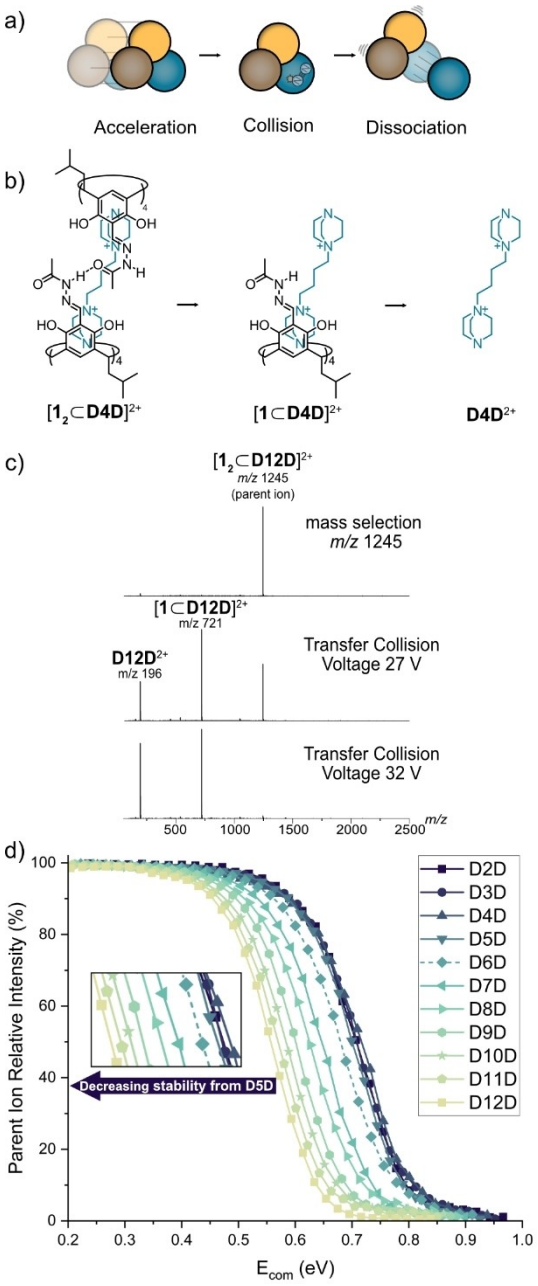

Figure 2. a) Principles of CID where the ions are accelerated into an inert collision gas converting kinetic energy into internal energy of the ion. Dissociation of the ion will follow if the internal energy is sufficiently high. b) Representative fragmentation pathway of $[\mathbf{1_2}\subset\mathbf{D4D}]^{2+}$ ion, which was also seen for the other hosts and guests with $n \leq 3$. c) CID spectra for $[\mathbf{1_2}\subset\mathbf{D12D}]^{2+}$, measurements performed on a Synapt G2-S in the transfer cell with N_2 as collision gas. d) SY curves of $[\mathbf{1_2}\subset\mathbf{DnD}]^{2+}$ with a zoom of the $SY_{50\%}$ region shown in the inset. Note that the collision voltage was converted to the centre of mass energy (E_{com}) as described in the Supporting Information.

(Figure 2d). The same trend was also observed for $\mathbf{2_2}$, but the stability decreases from $n=7$ (Figure S28), reflecting the larger cavity of $\mathbf{2_2}$ compared to $\mathbf{1_2}$.

The CID results indicate guest encapsulation even for those **DnD** longer than the cavity. A possible explanation for the encapsulation of these guests is a rupturing of the intermolecular hydrogen bonding between the cavitands with the guest

bridging the two partially or completely separated monomers (Figure 3a). To investigate this, measurements were performed with an N,N-dimethylhydrazone derivative (**3**) (Figure 3b) which cannot form intermolecular hydrogen bonds so can only dimerise via a bridging guest. In contrast to $\mathbf{1}_2$ and $\mathbf{2}_2$, $[\mathbf{3}_2+\mathbf{DnD}]^{2+}$ ions were only observed for $n \geq 5$ indicating that dimeric complexes with shorter guests are not very stable. SY analysis of $[\mathbf{3}_2+\mathbf{DnD}]^{2+}$ showed *increasing* stability with guest length until **D10D** where a plateau was reached (Figure 3c). This stability trend is expected for a complex in which no additional interactions between host cavitands exist where very short guests can only bridge the two monomers with destabilizing steric clashes between them. The steric clashes reduce with medium-sized guests permitting dimer formation. This becomes energetically more favourable with guest length until a threshold distance is reached where the two monomers are fully separated so that stability does not change anymore with longer guests. The fact that the inverse trend is observed for $\mathbf{3}_2$ suggests $\mathbf{1}_2$ and $\mathbf{2}_2$ are maintaining hydrogen bonding between the cavitands in some manner (Figure 3d).

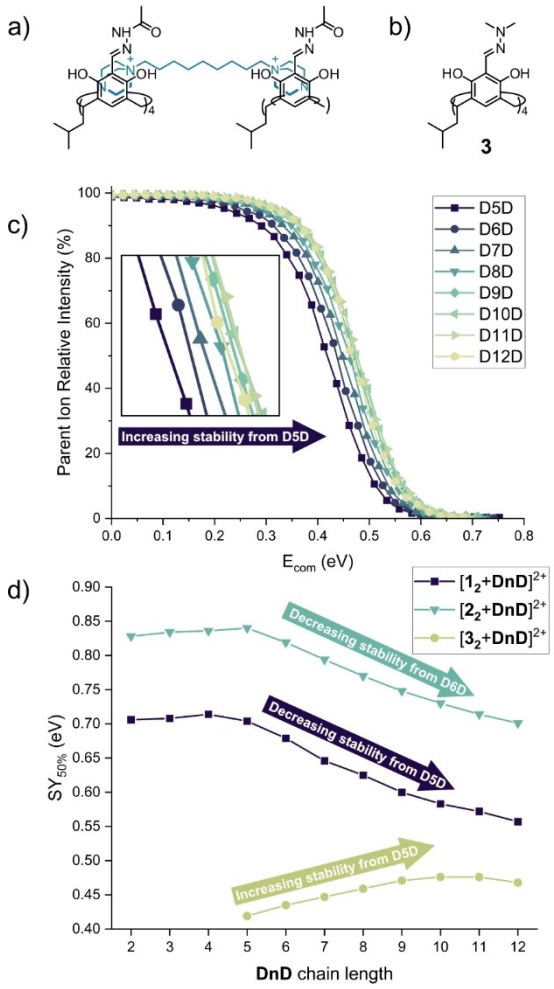

Figure 3. a) Potential non-hydrogen-bonded dimer where a **DnD** bridges across the two cavitands. b) N,N-dimethylhydrazoneresorcinarene (**3**). c) SY curves of $[\mathbf{3}_2+\mathbf{DnD}]^{2+}$ with n = 5–12. A zoom of the $SY_{50\%}$ region of the curves is shown in the inset. CID measurements performed on a Synapt G2-S in the transfer cell with N_2 as collision gas. Note that the collision voltage was converted to the centre of mass energy (E_{com}) as described in the Supporting Information. d) Plot of collected $SY_{50\%}$ of $[M_2+\mathbf{DnD}]$ for $\mathbf{1}_2$, $\mathbf{2}_2$, $\mathbf{3}_2$. This is done to visualise the stability trends of the hosts but the kinetic shift differences are too large to make a reliable direct comparison between them.

An explanation for encapsulation, while maintaining hydrogen bonding between the cavitands, would involve distortion of the guests from their fully extended form to fit inside the cavity. It has been demonstrated in solution that alkane guests can bind inside resorcinarene capsules by coiling into a helical arrangement.[27] If a similar coiling is occurring here, the SY trends where longer guests destabilize the capsule can be rationalised by the strain associated with deviation from the ideal guest geometry in addition to the increased charge repulsion at the reduced distance. Guest coiling can be monitored via gas-phase hydrogen/deuterium exchange (HDX) experiments which can be conducted with a Fourier-Transform Ion-Cyclotron-Resonance (FTICR) mass spectrometer. FTICRs allow precise control of reaction intervals with both the number and rate of exchange(s) being structurally informative.[28] HDX will shift from a fast concerted, Grotthus-like mechanism, to a slower non-concerted process that involves unfavourable charge separation species when a continuous hydrogen-bonding seam that runs around the capsule is disrupted (Figure S29).[29] The hydrogen bonding pattern of $\mathbf{1}_2$ would be expected to remain intact if the guests are coiling inside the cavity, and thus should produce similar HDX results with all guests. In the series of $[\mathbf{1}_2\subset\mathbf{DnD}]^{2+}$ ions, irrespective of the encapsulated guest, up to 24 exchanges were observed corresponding to the 8 N–H and 16 O–H hydrogens (Figures 4a and S30). However, the rate of exchange continually decreased from n = 5 onwards, correlating closely to the CID results, and suggests guest binding modes which impact the N–H···O bonds between the strands. The HDX indicates that smaller guests allow the capsule to form a fully closed, non-disrupted seam which results in fast exchange whilst for the intermediate-sized guests, the seam is opened occasionally due to steric clash with the guests reducing the exchange rate. The rate further slows with the longer guests as they have a constantly partially open seam preventing efficient exchange.

These situations can be distinguished from each other with the orthogonal technique of IMS which provides structural information by separating ions based on their size and shape.[30] Simply speaking, IMS acts as a wind tunnel for ions by transmitting them through a drift cell filled with an inert drift gas where low-energy collisions with the drift gas decelerates the ions resulting in different arrival times at the detector. The collision cross section (CCS) of an ion is its effective area that will undergo collisions with the drift gas and is thus a molecular property related to size and shape. CCS will influence the arrival time of an ion as a smaller ion will undergo fewer collisions and will have a shorter arrival time than a larger ion experiencing more collisions.[31] Arrival time will also be dependent on an ion's charge as well as instrumental conditions, but, for ions of the of the same charge measured under the same conditions, arrival times can be directly compared to assess relative size differences. For host-guest systems, IMS can be used to infer conformational differences as well as guest binding modes.[32]

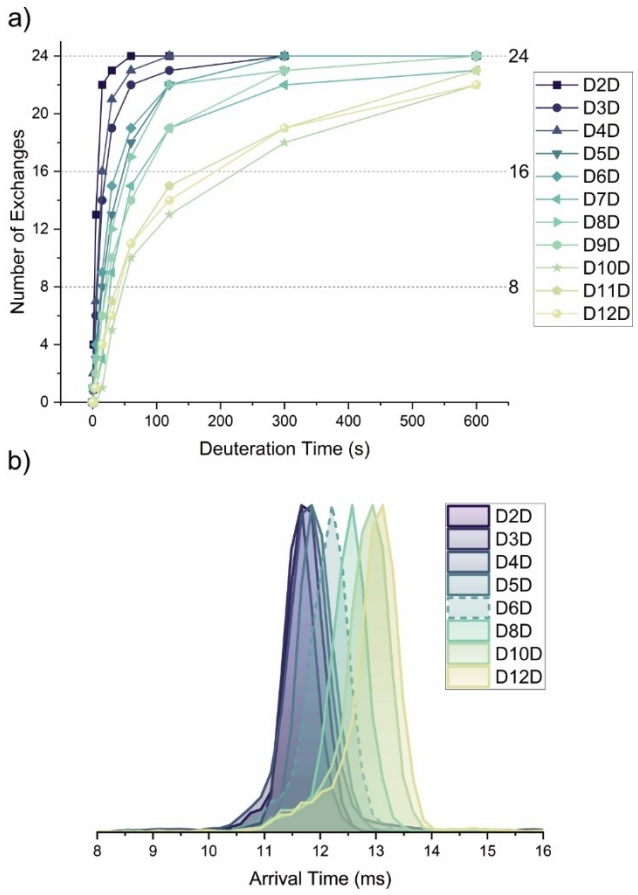

Figure 4. a) HDX for $[\mathbf{1}_2\subset\mathbf{DnD}]^{2+}$. The dashed lines represent the 8 NH and 16 OH which are exchangeable. The number of exchanges is consistent, but the rate decreases for longer guests; b) Arrival time distributions of $[\mathbf{1}_2\subset\mathbf{DnD}]^{2+}$ for n = 2–6,8,10,12 n = 7,9,11 omitted for clarity. Measurements performed on a Synapt G2-S with N_2 as buffer gas.

When considering space-filling models of both $\mathbf{1}_2$ and $\mathbf{2}_2$ (Figure S31), they show an almost non-porous structure and thus non-disrupted systems encapsulating the guests would have similar CCS, and hence arrival times. Consequently, short guests which are encapsulated without disrupting the hydrogen bonding seam should all have comparable arrival times in IMS. Measurements of the $[\mathbf{1}_2\subset\mathbf{DnD}]^{2+}$ ions show similar arrival times for $n \leq 5$ with gradual increases in arrival time beyond this guest length (Figure 4b). These results, like HDX, also support the idea of a completely intact hydrogen bonding seam for the shorter guests which is then disrupted by the medium to long guests increasing arrival times. Comparable IMS results were also obtained for $\mathbf{2}_2$ (Figure S32), but again shifted to the next larger guest in the series, consistent with the larger cavity. For **3**, a size increase was apparent for all guests with only slight increases seen for longer guests (Figure S33). In all cases, there is good agreement between the onset of size increases seen in IMS with the decreases in stability seen via CID.

The experimental results all correlate well to one another providing a consistent picture for all hosts. Computational modelling was then used to further explore the complexes (Figure 5). Such large systems make full DFT calculation computationally expensive, so final structures were optimised using the HF-3c level of theory implemented in the ORCA software.[18] HF-3c incorporates the D3 dispersion corrections and offers a nice balance between accuracy and cost while being suitable for the analysis of host-guest systems.[33] The computational models of the different complexes provided structures and binding modes in line with all the observed results. As the charges on the guests are more localised on the inner nitrogen atoms, maximum cation-π interactions can be achieved by pointing these nitrogens into the resorcinarene cores (Figures 5a and S34). As **3** does not benefit from any interaction between cavitands, it can interact with the fully extended guests with no penalty resulting in acute angles between **D12D** and the upper rims of the resorcinarenes. Such an arrangement is not possible for the shorter **D5D** due to potential steric clashes of the two cavitands forcing a more head on arrangement with a larger binding angle. The angle between the guest and the second resorcinarene decreases with longer guests and this binding mode in addition to decreasing steric and Coulomb repulsion, can explain the stability trends seen via SY analysis (Figure 3b). The longer guests also account for the continual increase in arrival time seen in IMS (Figure S33), with the size convergence representing the point where the two resorcinarenes are parallel and pseudo-encapsulating the guests.

In $\mathbf{1}_2$, the guests also maximise cation-π interactions by pointing their inner nitrogens towards the electron-rich resorcinarene cores. The intermolecular N–H···O hydrogen bonds between the strands prevent the simple translation of the two resorcinarenes (as with **3**) so, to be able to maintain cation-π interactions, the two DABCOniums are effectively locked in position. Consequently, the carbon chain of the guest is forced to loop into a horseshoe-like arrangement (Figures 5b and S35). When the loop gets larger, it pushes against the strands of the host leading to a gradual weakening and eventual breaking of the H-bonds. Such weakening was first apparent with **D5D** which begins to strain the hydrogen bonds but allows the resorcinarene to reposition so that cation-π bonding is enhanced. The interplay between the weakening H-bonding and stronger cation-π interactions can account for the similar stabilities of **D2D**–**D5D**. Beyond **D5D**, longer guests continue to expand out of the cavity with the remaining H-bonds on the capsule effectively acting as a hinge to allow the portal to open further. This accounts for the observed stability trend seen in the SY plots as the hydrogen bonding on the strands near the guest loop continues to weaken when the loop grows. It would also decrease the HDX rate as the exchange begins to require a rearrangement which becomes more extreme with longer guests. Furthermore, as the strand is pushed away and the guests begin to expand outside the cavity, the CCS of the ion increases which contributes to the longer arrival times seen in IMS. IMS also has the benefit of being able to link computationally generated model compounds to experimental results via the calculation of both experimental CCS values ($^{TW}CCS_{N2}$) from the arrival times via a calibrant and theoretical CCS values ($^{TM}CCS_{N2}$) of computational

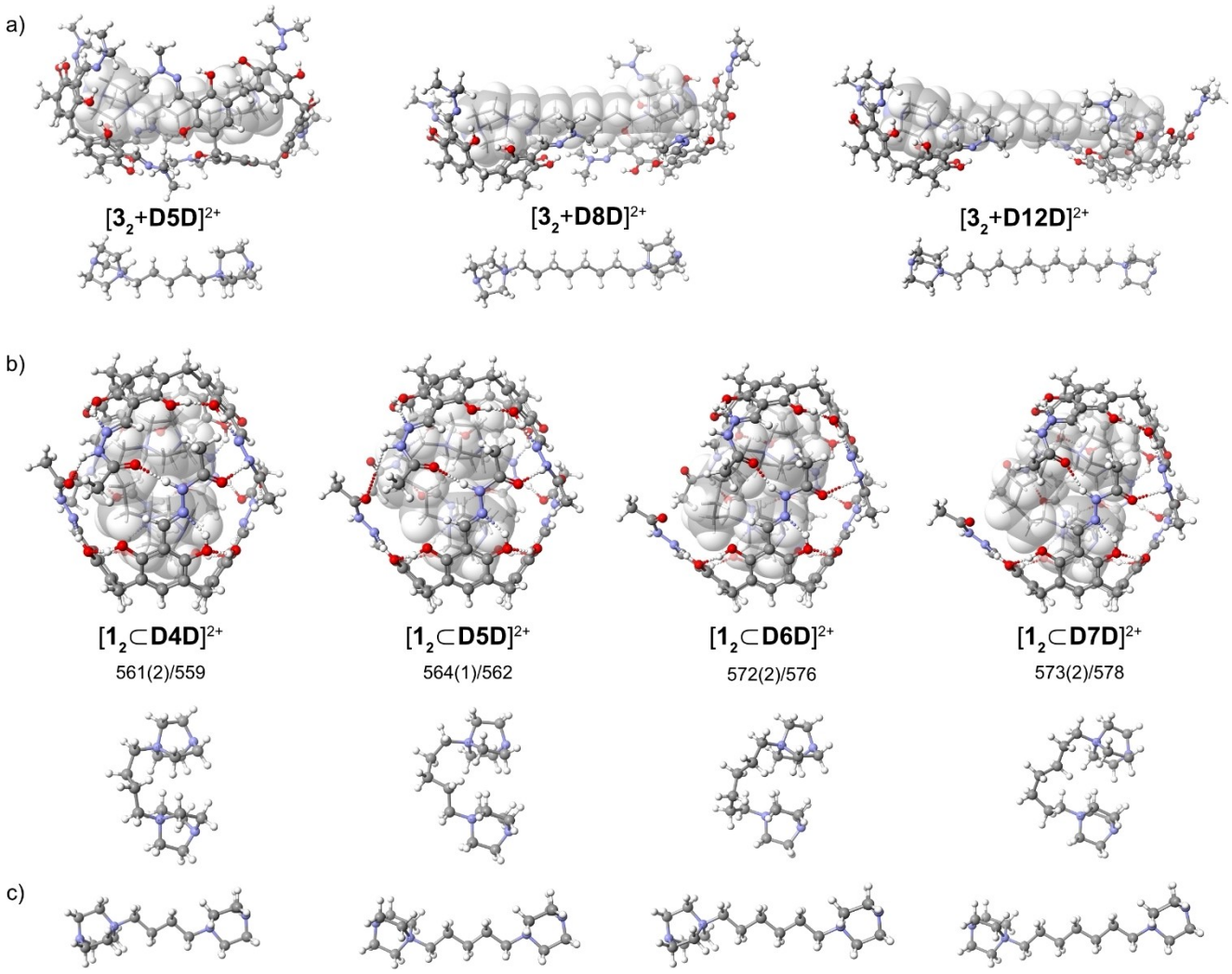

Figure 5. a) HF-3c optimised structures of: $[\mathbf{3_2}+\mathbf{DnD}]^{2+}$ with n = 5, 8, 12 (left to right). b) HF-3c optimised structures of $[\mathbf{1_2}\subset\mathbf{DnD}]^{2+}$ with n = 4, 5, 6, 7 (left to right), experimental $^{TW}CCS_{N2}$ values from CCS calibration (with standard deviation in parentheses) and theoretical $^{TM}CCS_{N2}$ values (as noted in the supplementary material) are given below the $[\mathbf{1_2}\subset\mathbf{DnD}]^{2+}$ structures. The bound guest is shown in space-filling mode in the host-guest structures and also shown without host underneath the respective host-guest structures. The *i-Bu* groups of the hosts have been omitted for clarity c) HF-3c optimised structures of free **D4**–**7D** (left to right) for comparison. The geometries of the bound guests within $\mathbf{1_2}$ deviates significantly from those of the free guests.

models of $\mathbf{1_2}$ (Figure 5b and Table S3) which in this case have good agreement with one another.[34] Taken together, the theoretical and experimental studies provide consistent results and strongly support the proposed binding mode of the **DnD** guests. These surprising binding modes represent a large deviation from the guest's preferred geometry (up to 16 Å, Figure 5c, Table S4) against a Coulomb barrier and require rearrangement of the host to accommodate. Such a strained conformation persists in the gas-phase due to the strengthening of the non-covalent interactions that hold it together.

Conclusions

In conclusion, we have shown the ability of ESI to generate host-guest complexes which cannot be observed in solution. This is possible as the shrinking charged droplets formed during ESI offer an environment where concentration increases, and ion pairing is obviated representing supramolecular chemistry occurring under conditions violating electroneutrality and reveals the intriguing chemistry that can result.

Using this strategy, guests too long for the cavity can be encapsulated in hydrogen-bonded resorcinarene capsules producing unusual conformations. The structures are assigned in the gas-phase with three structure-indicative MS techniques, CID, IMS and HDX which show decreasing stability above certain guest lengths and indicate guest expansion outside of the cavity for longer guests. The experimental results are coherent with one another and have been validated by computational modelling which reveals guests distorting into a horse-shoe arrangement upon encapsulation. This requires a large deviation of the guests from their ideal geometry in addition to distortions of the host, producing "spring-loaded" capsules with conformations that would be difficult to predict.

These complexes survive in the gas-phase, overcoming steric strain and the charge repulsion between the two DABCOnium moieties, due to the strengthening of the non-covalent interactions in the absence of solvent enabling investigation with MS. The ability of MS to unravel the conformation of these complexes is important as MS is uniquely positioned to study the chemistry occurring in these charged droplets. We envisage that many unique binding motifs can be generated in this manner which can be studied by MS.

Supporting Information

The authors have cited additional references within the Supporting Information.[35]

Acknowledgements

We thank the European Union through the NOAH project (H2020-MSCA-ITN project Ref. [76]5297) and FU Berlin for funding. Support for measurements by the BioSupraMol core facility at FU Berlin is gratefully acknowledged. Fei Jia is acknowledged for providing some of the guests used for initial measurements. We are grateful to Janos Wasternack for the NaBArF salt and to Sebastian Müller for synthesising it and acknowledge the members of the Szumna group and IChO staff for their support during the secondment of DLS in Warsaw. Thank you to Marek Szymański for help with the synthesis of **2**. Open Access funding enabled and organized by Projekt DEAL.

Conflict of Interests

The authors declare no conflict of interest.

Data Availability Statement

The data that support the findings of this study are available from the corresponding author upon reasonable request.

Keywords: charged droplets · electrospray ionisation · host-guest systems · mass spectrometry · resorcinarenes

[1] a) M. Wilm, *Mol. Cell. Proteomics* **2011**, *10*, M111.009407; b) P. Kebarle, L. Tang, *Anal. Chem.* **1993**, *65*, A972–A986; c) J. B. Fenn, *Angew. Chem. Int. Ed.* **2003**, *42*, 3871–3894; d) G. L. Glish, R. W. Vachet, *Nat. Rev. Drug Discovery* **2003**, *2*, 140–150.
[2] a) X. Yan, R. M. Bain, R. G. Cooks, *Angew. Chem. Int. Ed.* **2016**, *55*, 12960–12972; b) M. Girod, E. Moyano, D. I. Campbell, R. G. Cooks, *Chem. Sci.* **2011**, *2*, 501–510.
[3] N. K. Beyeh, M. Kogej, A. Åhman, K. Rissanen, C. A. Schalley, *Angew. Chem. Int. Ed.* **2006**, *45*, 5214–5218.
[4] a) J. Seo, S. Warnke, K. Pagel, M. T. Bowers, G. von Helden, *Nat. Chem.* **2017**, *9*, 1263–1268; b) S. Vandenbussche, G. Vandenbussche, J. Reisse, K. Bartik, *Eur. J. Org. Chem.* **2006**, *2006*, 3069–3073; c) D. P. Weimann, C. A. Schalley, *Supramol. Chem.* **2008**, *20*, 117–128.
[5] S. C. Nanita, R. G. Cooks, *Angew. Chem. Int. Ed.* **2006**, *45*, 554–569.
[6] J. Mehara, J. Roithová, *Chem. Sci.* **2020**, *11*, 11960–11972.
[7] L. Cera, C. A. Schalley, *Chem. Soc. Rev.* **2014**, *43*, 1800–1812.
[8] a) H.-J. Schneider, U. Schneider, *J. Incl. Phenomena Mol. Rec.* **1994**, *19*, 67–83; b) K. Kobayashi, M. Yamanaka, *Chem. Soc. Rev.* **2015**, *44*, 449–466.
[9] K. N. Rose, L. J. Barbour, G. W. Orr, J. L. Atwood, *Chem. Commun.* **1998**, 407–408.
[10] a) C. Gaeta, C. Talotta, M. De Rosa, P. La Manna, A. Soriente, P. Neri, *Chem. Eur. J.* **2019**, *25*, 4899–4913; b) M. Yamanaka, A. Shivanyuk, J. Rebek, Jr., *J. Am. Chem. Soc.* **2004**, *126*, 2939–2943; c) S. Gambaro, M. De Rosa, A. Soriente, C. Talotta, G. Floresta, A. Rescifina, C. Gaeta, P. Neri, *Org. Chem. Front.* **2019**, *6*, 2339–2347.
[11] a) T. Heinz, D. M. Rudkevich, J. Rebek, Jr., *Nature* **1998**, *394*, 764–766; b) H. Mansikkamäki, M. Nissinen, K. Rissanen, *Chem. Commun.* **2002**, 1902–1903.
[12] a) W.-Y. Pei, G. Xu, J. Yang, H. Wu, B. Chen, W. Zhou, J.-F. Ma, *J. Am. Chem. Soc.* **2017**, *139*, 7648–7656; b) R. Pinalli, V. Cristini, V. Sottili, S. Geremia, M. Campagnolo, A. Caneschi, E. Dalcanale, *J. Am. Chem. Soc.* **2004**, *126*, 6516–6517.
[13] a) M. Chwastek, P. Cmoch, A. Szumna, *Angew. Chem. Int. Ed.* **2021**, *60*, 4540–4544; b) M. Chwastek, P. Cmoch, A. Szumna, *J. Am. Chem. Soc.* **2022**, *144*, 5350–5358.
[14] a) N. K. Beyeh, F. Pan, K. Rissanen, *Angew. Chem. Int. Ed.* **2015**, *54*, 7303–7307; b) O. Dumele, N. Trapp, F. Diederich, *Angew. Chem. Int. Ed.* **2015**, *54*, 12339–12344.
[15] a) D. Ajami, J. Rebek, Jr., *J. Am. Chem. Soc.* **2006**, *128*, 5314–5315; b) D. Ajami, J. Rebek, Jr., *Angew. Chem. Int. Ed.* **2007**, *46*, 9283–9286.
[16] S. S. Zhu, H. Staats, K. Brandhorst, J. Grunenberg, F. Gruppi, E. Dalcanale, A. Lützen, K. Rissanen, C. A. Schalley, *Angew. Chem. Int. Ed.* **2008**, *47*, 788–792.
[17] a) M. Szymański, M. Wierzbicki, M. Gilski, H. Jędrzejewska, M. Sztylko, P. Cmoch, A. Shkurenko, M. Jaskólski, A. Szumna, *Chem. Eur. J.* **2016**, *22*, 3148–3155; b) M. P. Szymański, J. S. Czajka, P. Cmoch, W. Iwanek, A. Szumna, *Supramol. Chem.* **2018**, *30*, 430–437.
[18] a) R. Sure, S. Grimme, *J. Comput. Chem.* **2013**, *34*, 1672–1685; b) F. Neese, *WIREs Comput. Mol. Sci.* **2012**, *2*, 73–78; c) F. Neese, *WIREs Comput. Mol. Sci.* **2022**, *12*, e1606.
[19] H. Mansikkamäki, C. A. Schalley, M. Nissinen, K. Rissanen, *New J. Chem.* **2005**, *29*, 116–127.
[20] R. J. Hooley, S. M. Biros, J. Rebek, Jr., *Chem. Commun.* **2006**, 509–510.
[21] B. Wüstenberg, A. Pfaltz, *Adv. Synth. Catal.* **2008**, *350*, 174–178.
[22] P. Kebarle, U. H. Verkerk, *Mass Spectrom. Rev.* **2009**, *28*, 898–917.
[23] a) L. Sleno, D. A. Volmer, *J. Mass Spectrom.* **2004**, *39*, 1091–1112; b) M. Rodgers, K. M. Ervin, P. B. Armentrout, *J. Chem. Phys.* **1997**, *106*, 4499–4508.
[24] C. A. Schalley, C. Verhaelen, F.-G. Klärner, U. Hahn, F. Vögtle, *Angew. Chem. Int. Ed.* **2005**, *44*, 477–480.
[25] T. Heravi, J. Shen, S. Johnson, M. C. Asplund, D. V. Dearden, *J. Phys. Chem. A* **2021**, *125*, 7803–7812.
[26] a) M. W. Forbes, D. A. Volmer, G. J. Francis, D. K. Böhme, *J. Am. Soc. Mass Spectrom.* **2005**, *16*, 779–791; b) T. M. Kertesz, L. H. Hall, D. W. Hill, D. F. Grant, *J. Am. Soc. Mass Spectrom.* **2009**, *20*, 1759–1767; c) N. Geue, T. S. Bennett, A.-A.-M. Arama, L. A. I. Ramakers, G. F. S. Whitehead, G. A. Timco, P. B. Armentrout, E. J. L. McInnes, N. A. Burton, R. E. P. Winpenny, P. E. Barran, *J. Am. Chem. Soc.* **2022**, *144*, 22528–22539; d) F. Schwer, S. Zank, M. Freiberger, R. Kaur, S. Frühwald, C. C. Robertson, A. Görling, T. Drewello, D. M. Guldi, M. von Delius, *Organic Materials* **2022**, *4*, 7–17.
[27] a) D. Ajami, J. Rebek, Jr., *J. Am. Chem. Soc.* **2006**, *128*, 15038–15039; b) D. Ajami, J. Rebek, Jr., *Nat. Chem.* **2009**, *1*, 87–90; c) F. U. Rahman, R. Wang, H. B. Zhang, O. Brea, F. Himo, J. Rebek Jr, Y. Yu, *Angew. Chem. Int. Ed.* **2022**, *61*, e202205534.
[28] a) H. D. F. Winkler, E. V. Dzyuba, C. A. Schalley, *New J. Chem.* **2011**, *35*, 529–541; b) K. D. Rand, S. D. Pringle, J. P. Murphy, K. E. Fadgen, J. Brown, J. R. Engen, *Anal. Chem.* **2009**, *81*, 10019–10028; c) M. E. Hemling, J. J. Conboy, M. F. Bean, M. Mentzer, S. A. Carr, *J. Am. Soc. Mass Spectrom.* **1994**, *5*, 434–442; d) M. A. Freitas, C. L. Hendrickson, M. R. Emmett, A. G. Marschall, *Int. J. Mass Spectrom.* **1999**, *185/186/187*, 565–575.
[29] H. D. F. Winkler, E. V. Dzyuba, J. A. W. Sklorz, N. K. Beyeh, K. Rissanen, C. A. Schalley, *Chem. Sci.* **2011**, *2*, 615–624.
[30] a) A. B. Kanu, P. Dwivedi, M. Tam, L. Matz, H. H. Hill, *J. Mass Spectrom.* **2008**, *43*, 1–22; b) F. Lanucara, S. W. Holman, C. J. Gray, C. E. Eyers, *Nat. Chem.* **2014**, *6*, 281–294.
[31] E. Christofi, P. Barran, *Chem. Rev.* **2023**, *123*, 2902–2949.
[32] a) E. Kalenius, M. Groessl, K. Rissanen, *Nat. Chem. Rev.* **2019**, *3*, 4–14; b) A. Kruve, K. Caprice, R. Lavendomme, J. M. Wollschläger, S. Schoder,

H. V. Schröder, J. R. Nitschke, F. B. Cougnon, C. A. Schalley, *Angew. Chem. Int. Ed.* **2019**, *58*, 11324–11328; c) E. Hanozin, B. Mignolet, J. Martens, G. Berden, D. Sluysmans, A. S. Duwez, J. F. Stoddart, G. Eppe, J. Oomens, E. De Pauw, D. Morsa, *Angew. Chem. Int. Ed.* **2021**, *60*, 10049–10055; d) S. Ibáñez, C. Vicent, E. Peris, *Angew. Chem. Int. Ed.* **2022**, *61*, e202112513; e) C.-W. Chu, D. L. Stares, C. A. Schalley, *Chem. Commun.* **2021**, *57*, 12317–12320; f) M. C. Pfrunder, D. L. Marshall, B. L. Poad, T. M. Fulloon, J. K. Clegg, S. J. Blanksby, J. C. McMurtrie, K. M. Mullen, *Angew. Chem. Int. Ed.* **2023**, *62*, e202302229.

[33] a) S. Grimme, S. Ehrlich, L. Goerigk, *J. Comput. Chem.* **2011**, *32*, 1456–1465; b) V. K. Prasad, A. Otero-de-la-Roza, G. A. DiLabio, *J. Chem. Theory Comput.* **2022**, *18*, 2208–2232; c) R. Sure, S. Grimme, *J. Chem. Theory Comput.* **2015**, *11*, 3785–3801; d) J. G. Brandenburg, M. Hochheim, T. Bredow, S. Grimme, *J. Phys. Chem. Lett.* **2014**, *5*, 4275–4284; e) M. Bursch, J.-M. Mewes, A. Hansen, S. Grimme, *Angew. Chem. Int. Ed.* **2022**, *61*, e202205735.

[34] U. Warzok, M. Marianski, W. Hoffmann, L. Turunen, K. Rissanen, K. Pagel, C. A. Schalley, *Chem. Sci.* **2018**, *9*, 8343–8351.

[35] a) M. Grajda, M. Wierzbicki, P. Cmoch, A. Szumna, *J. Org. Chem.* **2013**, *78*, 11597–11601; b) F. Jia, Z. He, L.-P. Yang, Z.-S. Pan, M. Yi, R.-W. Jiang, W. Jiang, *Chem. Sci.* **2015**, *6*, 6731–6738; c) Z. He, G. Ye, W. Jiang, *Chem. Eur. J.* **2015**, *21*, 3005–3012; d) M. Gaedke, H. Hupatz, F. Witte, S. M. Rupf, C. Douglas, H. V. Schröder, L. Fischer, M. Malischewski, B. Paulus, C. A. Schalley, *Org. Chem. Front.* **2022**, *9*, 64–74; e) P. Mal, B. Breiner, K. Rissanen, J. R. Nitschke, *Science* **2009**, *324*, 1697–1699; f) A. Shivanyuk, J. Rebek, Jr., *Proc. Natl. Acad. Sci. USA* **2001**, *98*, 7662–7665; g) A. Scarso, L. Trembleau, J. Rebek, Jr., *Angew. Chem. Int. Ed.* **2003**, *42*, 5499–5502; h) M. F. Bush, Z. Hall, K. Giles, J. Hoyes, C. V. Robinson, B. T. Ruotolo, *Anal. Chem.* **2010**, *82*, 9557–9565; i) V. Shrivastav, M. Nahin, C. J. Hogan, C. Larriba-Andaluz, *J. Am. Soc. Mass Spectrom.* **2017**, *28*, 1540–1551; j) D. P. Weimann, H. D. F. Winkler, J. A. Falenski, B. Koksch, C. A. Schalley, *Nat. Chem.* **2009**, *1*, 573–577; k) K. M. Ervin, P. B. Armentrout, *J. Chem. Phys.* **1985**, *83*, 166–189.

Manuscript received: July 3, 2023
Accepted manuscript online: September 19, 2023
Version of record online: October 31, 2023